World Journal of

Radiology

World Journal of *Radiology*

Contents

Contents

ABOUT COVER

Editorial Board Member of *World Journal of Radiology*, Vlastimil Valek, MD, PhD, Professor, Department of Radiology, University Hospital Brno, Brno 62800, Czech Republic

AIM AND SCOPE

World Journal of Radiology (*World J Radiol*, *WJR*, online ISSN 1949-8470, DOI: 10.4329) is a peer-reviewed open access academic journal that aims to guide clinical practice and improve diagnostic and therapeutic skills of clinicians.

WJR covers topics concerning diagnostic radiology, radiation oncology, radiologic physics, neuroradiology, nuclear radiology, pediatric radiology, vascular/interventional radiology, medical imaging achieved by various modalities and related methods analysis. The current columns of *WJR* include editorial, frontier, diagnostic advances, therapeutics advances, field of vision, mini-reviews, review, topic highlight, medical ethics, original articles, case report, clinical case conference (clinicopathological conference), and autobiography.

We encourage authors to submit their manuscripts to *WJR*. We will give priority to manuscripts that are supported by major national and international foundations and those that are of great basic and clinical significance.

INDEXING/ABSTRACTING

World Journal of Radiology is now indexed in PubMed, PubMed Central, and Emerging Sources Citation Index (Web of Science).

EDITORS FOR THIS ISSUE

Retrospective Study

Evaluation of pineal cysts with magnetic resonance imaging

Erkan Gokce, Murat Beyhan

Erkan Gokce, Department of Radiology, Gaziosmanpaşa University, School of Medicine, Tokat 60100, Turkey

Murat Beyhan, Department of Radiology, Tokat State Hospital, Tokat 60100, Turkey

ORCID number: Erkan Gokce (0000-0002-1809-2172); Murat Beyhan (0000-0002-8630-4632).

Correspondence to: Erkan Gokce, MD, Associate Professor, Department of Radiology, Gaziosmanpaşa University, School of Medicine, Kaleardı Quarter, Muhittin Fisunoglu Street, Tokat 60100, Turkey. erkangokce@mynet.com

Telephone: +90-542-3798986
Fax: +90-362-2309105

Abstract

AIM

To evaluate radiological imaging findings of patients who had been found to have pineal cyst (PC) in brain magnetic resonance imaging (MRI).

METHODS

A total of 9546 patients who had brain MRI examination in March 2010-January 2018 period were studied. Fifty-six patients (44 female and 12 male) found to have PC were evaluated. Eighteen of the patients had had follow-up examinations of 2-94 mo (mean 30.50 ± 28.83). PC dimensions and volume, radiological imaging features (signal intensities, contours, internal septation-loculation and contrast-enhancement features) and natural history in cases who had been followed-up were evaluated by two radiologists.

RESULTS

Of 9546 patients, 5555 were female (58.2%) and 3991 male (41.8%). Age range was 1-99 (mean 43.18 ± 20.94). PC frequency was calculated to be 0.58%. Forty-four of the 56 patients (78.57%) with PC were female and 12 male (21.43%), and their age range was 5-61 (mean 31.26 ± 12.73). Thirty-five of the PCs were typical (62.50%) and 21 (37.50%) were atypical. No significant difference was found between initial and final imaging sizes of PCs which were monitored by follow-up examinations (*P* > 0.05).

CONCLUSION

PCs are cysts which do not show clear size and natural changes and are more frequently observed in females and in adult ages. Most of them are isointense with cerebrospinal fluid on T1 and T2A weighted images, hyperintense compared to cerebrospinal fluid on fluid-attenuated inversion recovery; sequence and smoothly contoured. Their typical forms have peripheral rim and multilocular ones may have septal contrast-enhancement.

Key words: Magnetic resonance imaging; Pineal cyst; Pineal region

Core tip: In this retrospective study, brain magnetic resonance images of 9546 patients were studied to detect incidence, size, contour, septation and contrast-enhancement features of pineal cysts (PCs). In addition, size and natural changes in follow-up examinations were also investigated. Classification of PCs based on routine magnetic resonance imaging examinations could change when examination was performed using high resolution sequences due to detection of septations within them. The present study revealed that no significant size or natural change was observed in follow-up examinations of PCs.

INTRODUCTION

Pineal cysts (PC) are frequently asymptomatic, small sized, unilocular, benign pineal lesions which do not show size change[1]. They are generally made of three layers: fibrocollagen layer at the outside, pineal parenchymal layer which may have calcium deposits at the middle and hypocellular glial tissue layer which may have hemosiderin inside[1,2]. PCs may develop as secondary to focal degeneration of pineal gland or distension of pineal diverticulum remnant[3]. Increasing resolution and more frequent use of cranial imaging techniques along with use of contrast agent have led to an increase in incidental diagnosis of PCs[1]. Unilocular, smooth edged, round or ovoid shaped cysts which have homogenous interior signal feature and rim-shaped contrast-enhancement with less than 2 mm wall thickness on MRI are referred as typical PC[4,5]. Although there is an excess amount of reports in literature about typical PC stating that they are indeed incidental findings of radiological imaging and that they are stable over time, more complex and atypical pineal cystic lesions constitute a problem for radiologists[4-7].

In addition, it has been reported that pineal neoplasia could have imaging features similar to those of PC[5,8]. Some studies mentioned some cystic lesions in pineal region with complex imaging features, which are probably normal variants[5,9,10]. In the present study, radiological imaging findings of PCs determined in patients who had undergone brain magnetic resonance imaging (MRI) due to various reasons in a past eight-year period were evaluated.

MATERIALS AND METHODS

After the approval of local ethic committee (No. 18-KA-EK-015), 9546 patients who had brain MRI examinations in March 2010-January 2018 period in Radiology Department of Gaziosmanpaşa University Medical School were studied retrospectively. A total of 11695 consecutive brain MRI examinations were scanned. Scans were reviewed by experienced neuroradiologists (Gokce E and Beyhan M) to confirm radiologic diagnoses of PC. Patients with solid or semisolid masses in pineal gland location or other cystic lesions (arachnoid cyst, *etc*.) developing from neighboring structures and patients with operation history were excluded. There were no exclusion criteria related to pineal cyst size. Fifty-six patients (44 female and 12 male) with PCs were evaluated. Among the reasons for MRI requests were headache, cerebrovascular disease, epilepsy, vertigo, hand tremors and encephalitis. MRI examinations were carried out using an 8-channel 1.5 T MRI machine (GE Signa Excite HD; GE Healthcare, Milwaukee, WI, United States, 2005) until 2017, and a 16-channel 1.5 T MRI machine (GE Signa Explorer SV 25; GE Healthcare, Milwaukee, WI, United States, 2016) after 2017. MRI examination parameters before and after 2017 are given in Tables 1 and 2. Eighteen patients had 2-94 mo (mean 30.50 ± 28.83) of follow-ups. Contrast-enhanced MRI was performed in 21 of 56 patients.

Size and volume, radiological imaging features (signal intensities, contours, internal septation-loculation and contrast-enhancement properties) and size and natural changes of PCs (in patients who had follow-ups) were evaluated by two radiologists. PC dimensions were measured from outer wall to outer wall in sagittal, axial and coronal planes. Unilocular, smooth edged, ovoid PCs with homogenous interior structure and less than 2 mm wall thickness were considered typical PC (Figures 1-3), while multilocular PCs with walls thicker than 2 mm, septation or lobulated contours were considered atypical (Figures 4-10). In patients who had had follow-up examinations, size and natural differences were compared in initial and follow-up examinations.

Statistical analysis

Descriptive statistics were expressed as mean ± SD. Data regarding categorical variables were given as n (%). Categorical variables were compared using χ^2 tests. Independent-samples t-test and Mann-Whitney *U*

Table 1 Magnetic resonance imaging examination parameters before 2017

Parameter	T1 (SPGR)	T2 (SE)	FLAIR	DWI	Ax SPGR + C	Sag T1 SE + C	Ax T1 FS + C
TR (repetition time) (ms)	6.36	5700	8002	8000	6.36	440	620
TE (echo time) (ms)	2.23	134	80.9	104	2.23	12	20
Field of view (mm)	260	250	220	250	260	250	250
Slice thickness (mm)	4	5	5.5	5	4	5.5	5.5
Slice gap (mm)	2	6.5	6.5	6.5	2	6.5	7
NEX (No. of excitations)	1	1.5	1	2	1	1	1
TI (time inversion) ms	450		2000		450		
Machine	1.5 T GE Signa Excite HD (8 channel head coil)						

SPGR: Spoiled gradient recalled acquisition in steady state; SE: Spin echo; FLAIR: Fluid-attenuated inversion recovery; DWI: Diffusion weighted imaging; Ax: Axial plane; Sag: Sagittal plane; + C: Contrast-enhanced; FS: Fat saturation.

Table 2 Magnetic resonance imaging examination parameters after 2017

Parameter	T1 (BRAVO)	T2 (SE)	FLAIR FS	DWI	T1 (BRAVO) +C	Cor T1 (SE) + C	Ax T1 FS + C
TR (repetition time) (ms)	9.25	6282	10000	6992	9.25	3509	2744
TE (echo time) (ms)	3.58	124	91.7	84.4	3.58	17.8	17.5
Field of view (mm)	256	220	240	270	256	240	256
Slice thickness (mm)	1	5.5	5.5	5	1	5.5	5.5
Slice gap (mm)	0	7	7	5.5	0	7	7
NEX (No. of excitations)	1	2	1	2	1	1	1
TI (time inversion) (ms)	420		2688		420	1146	922
Machine	1.5 T GE Signa Explorer SV 25 (16 channel neurovascular-head coil)						

BRAVO: Brain volume imaging; SE: Spin echo; FLAIR: Fluid-attenuated inversion recovery; FS: Fat saturation; DWI: Diffusion weighted imaging; + C: Contrast-enhanced; Cor: Coronal plane; Ax: Axial plane.

Table 3 Demographic and clinical characteristics of patients with pineal cyst

Demographic and clinical characteristics	*n* (%)
No. of patients	56
Pineal cyst prevalence	0.58%
Median age (mean ± SD, range) (yr)	31.26 ± 12.73 (5–61)
Sex	
Female	44 (78.57)
Male	12 (21.43)
MRI request reasons	
Headache	42 (75)
Epilepsy	7 (12.50)
Cerebrovascular disease	4 (7.14)
Vertigo	1 (1.78)
Encephalitis	1 (1.78)
Hand tremor	1 (1.78)

MRI: Magnetic resonance imaging.

test were used to compare the means of two groups. The results of PC dimension measurements were compared using paired-samples *t*-test. A *P*-value of < 0.05 was considered significant. Statistical analyses were performed using the Statistical Package for Social Sciences 18.0 software (IBM Corp.; Armonk, NY, United States).

RESULTS

Studied brain MRI examinations belonged to 5555 women (58.2%) and 3991 men (41.8%), and the age range was 1-99 (mean 43.18 ± 20.94). Fifty-six patients were found to have had PC. Forty-four of them (78.57%) were female and 12 were men (21.43%). Calculated frequency of PC was 0.58%. Age range of patients with PC was 5-61 (mean: 31.26 ± 12.73). When the groups with and without PC were compared, a significant difference was found between the two groups for average age (*P* < 0.001). The difference between the genders for frequency of PC incidence was also significant (*P* = 0.002). The most common reason for MRI examination request was headache (42 patients). Demographic and clinical characteristics of patients with PC are given in Table 3.

One PC was slightly hyperintense on T2 weighed series compared to cerebrospinal fluid (CSF), but others were isointense (Figures 1-3). On T1 weighted series, three PCs were slightly hyperintense compared to CSF and other PCs were isointense. On fluid-attenuated inversion recovery (FLAIR) series, on the other hand, only six PCs were isointense with CSF, and others were hyperintense (Figure 2). No diffusion limitation was observed on diffusion MRI series in any PC (Figure 4). Contrast-enhancement was detected in PCs of all 21 patients who had undergone contrast-enhanced MRI examination. Vast majority of PC (71.42%) showed peripheral rim-like contrast-enhancement (Figure 1). However, peripheral rim-like contrast-enhancement and septal contrast-enhancement or partial rim style enhancement were less frequent (14.28% and 9.52%, respectively) (Figures 5, 7 and 10). One PC (4.76%)

Figure 1 Eighteen years old male patient with typical pineal cyst (patient No. 43). A: Axial plane T2 weighted magnetic resonance imaging (MRI); B: Sagittal plane T2 weighted MRI; C: Axial plane T1 weighted contrast-enhanced MRI; D: Sagittal plane contrast-enhanced MRI. Typical pineal cyst is shown in the pineal region with unilocular homogeneous internal structure (arrows, A, B, C and D); Peripheral rim-like contrast-enhancement is shown (arrow, C and D).

Figure 2 Thirty-three years old female patient with typical pineal cyst (patient No. 42). A: Axial plane T2 weighted magnetic resonance imaging (MRI); B: T1 weighted MRI; C: Sagittal plane T2 weighted MRI; D: Coronal plane FLAIR MRI. Typical pineal cysts are shown in the pineal region with unilocular homogeneous internal structure (white arrows, A, B, C and D); Isointense cyst with CSF (A, B and C); The slightly hyperintense pineal cyst compared to CSF is shown on FLAIR sequence (D). CSF: Cerebrospinal fluid; FLAIR: Fluid-attenuated inversion recovery.

Figure 3 Thirty-five years old female patient with typical pineal cyst (patient No. 34). A: Axial plane T2 weighted magnetic resonance imaging (MRI); B: T1 weighted MRI; C: Sagittal plane T2 weighted MRI; D: Coronal plane FLAIR MRI. Typical pineal cyst is shown in the pineal region with unilocular homogeneous internal structure (white arrows, A, B, C and D); The isointense pineal cyst compared to CSF is shown in the pineal region (A, B, C and D). CSF: Cerebrospinal fluid; FLAIR: Fluid-attenuated inversion recovery.

Figure 4 Fifty years old male patient with atypical pineal cyst (patient No. 40). Axial plane (A) sagittal plane magnetic resonance imaging (MRI) (B) coronal plane T2 weighted (C) and coronal plane FLAIR magnetic resonance imaging (D) axial plane diffusion weighted imaging (E) axial plane apparent diffusion coefficient map (F). A, B, C, D, E and F: Bilocular, lobule contoured atypical pineal cyst is shown in pineal area (white arrows); D: The slightly hyperintense pineal cyst compared to CSF is shown on FLAIR sequence; E and F: No diffusion restriction. CSF: Cerebrospinal fluid; FLAIR: Fluid-attenuated inversion recovery.

Figure 5 Fifty years old male patient with atypical pineal cyst (patient No. 40). Axial plane (A) sagittal plane T1 weighted (B) axial plane (C) sagittal plane contrast-enhanced magnetic resonance imaging (D). A, B, C and D: Bilocular, lobule contoured atypical pineal cyst is shown in pineal area (white arrows); C and D: Partial rim-like enhancement is shown (white arrows).

Figure 6 Thirty-six years old female patient with atypical pineal cyst (patient No. 2). Axial plane T2 weighted (A) sagittal plane (B) contrast-enhanced magnetic resonance imaging. A and B: Atypical pineal cysts are shown in the pineal region; A: Trilocular cyst (white arrow); B: Peripheral rim-like enhancement is shown (white arrow).

had intense heterogeneous contrast-enhancement, and complicated PC-pineocytoma differentiation could not be done radiologically (Figure 8). Most of the PCs were concluded to be typical (62.50%), while a smaller proportion was atypical (37.50%). Eighteen of the atypical PCs (32.4%) had two or more septation-loculation, and 11 (19.64%) had peripheral lobulation. Septation-loculation was observed in 9 (81.81%) of lobule-contoured PCs (Figure 9). MRI features of PCs are given in Table 4. Minimum and maximum PC diameters varied from 5.0 to 19.7 mm. Average PC sizes were 11.18 ± 3.03 mm in anteroposterior (AP), 10.41 ± 2.72 mm in mediolateral (ML) and 8.63 ± 2.47 mm in craniocaudal (CC) directions. Average PC volume was 0.62 ± 0.54 cm^3. A total of 18 PCs had follow-up examinations, and 10 of them were typical and 8 atypical. Natural change was not observed in any PCs with follow-ups. Amount of average dimension changes in PCs with follow-ups were (-0.08 ± 0.53) mm, (-0.22 ± 0.87) mm, and (0.16 ± 0.56) mm in AP, ML and CC dimensions, respectively. Thus, AP, ML and CC dimensions decreased in 6, 8 and 5 PCs, and increased in 5, 5 and 7 PCs, respectively. No significant difference was found between initial and final imaging sizes of

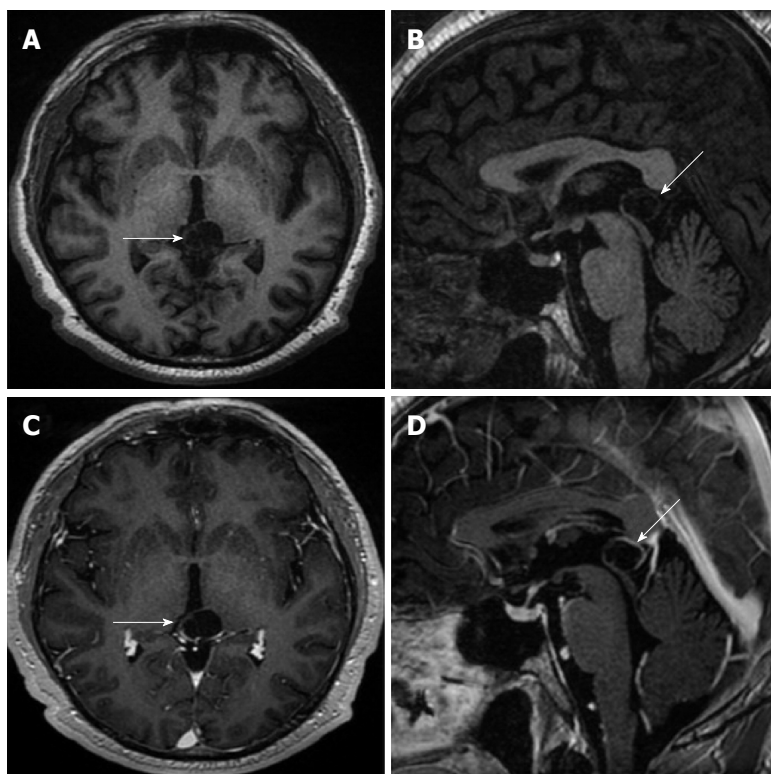**Figure 7 Thirty-three years old male patient with atypical pineal cyst (patient No. 41).** Axial plane (A) sagittal plane T2 weighted (B) coronal plane FLAIR (C) coronal plane (D) contrast-enhanced magnetic resonance imaging. A and B: Atypical multilocular pineal cysts are shown in the pineal region (white arrows); C: The hyperintense pineal cyst compared to CSF is shown in the pineal region (white arrows); D: Peripheral rim-like and septal enhancement is shown (white arrows). CSF: Cerebrospinal fluid; FLAIR: Fluid-attenuated inversion recovery.

Figure 8 Twenty-two years old female patient with atypical pineal cyst (patient No. 50). Axial plane T1 weighted (A) coronal plane FLAIR (B) axial plane diffusion weighted (C) consecutive contrast-enhanced magnetic resonance imaging (D, E and F). A, B, C, D, E and F: Atypical pineal cyst or pineocytoma is not distinguished radiologically (white arrows); C: No diffusion restriction; D, E and F: Increasing gradually heterogeneous enhancement is shown in pineal region (white arrows). FLAIR: Fluid-attenuated inversion recovery.

Figure 9 Thirty-three years old female patient with atypical pineal cyst (patient No. 53). Axial plane (A) T2 weighted (B) T1 weighted (C) contrast-enhanced (D) sagittal plane contrast-enhanced magnetic resonance imaging. A, B, C and D: Multilocular, lobule contoured, atypical pineal cyst is observed in pineal area (white arrows); C and D: Peripheral rim-like enhancement is shown (white arrows).
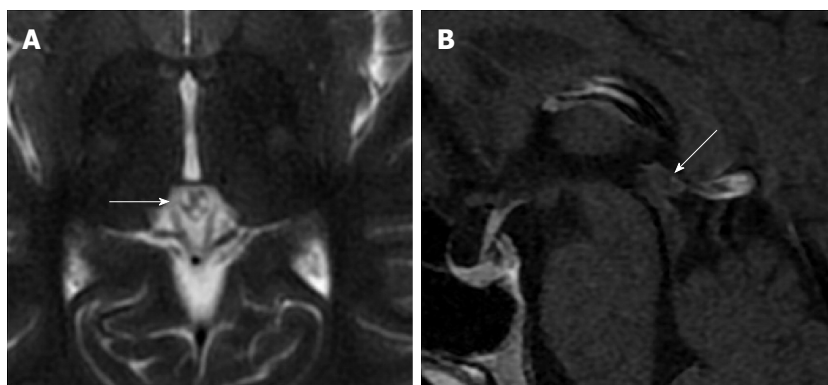

Figure 10 Five years old female patient with atypical pineal cyst (patient No. 44). Axial plane (A) T2 weighted (B) T1 weighted (C) sagittal plane T2 weighted (D) coronal plane FLAIR (E) axial plane (F) sagittal plane contrast-enhanced magnetic resonance imaging. A, B, C, D, E and F: Multilocular, lobule contoured, atypical pineal cyst is observed in pineal area (white arrows); D: The isointense pineal cyst compared to CSF is shown on FLAIR sequence; E and F: Peripheral rim-like and septal (white arrows) enhancement is shown. CSF: Cerebrospinal fluid; FLAIR: Fluid-attenuated inversion recovery.

Table 4 Magnetic resonance imaging features of pineal cysts

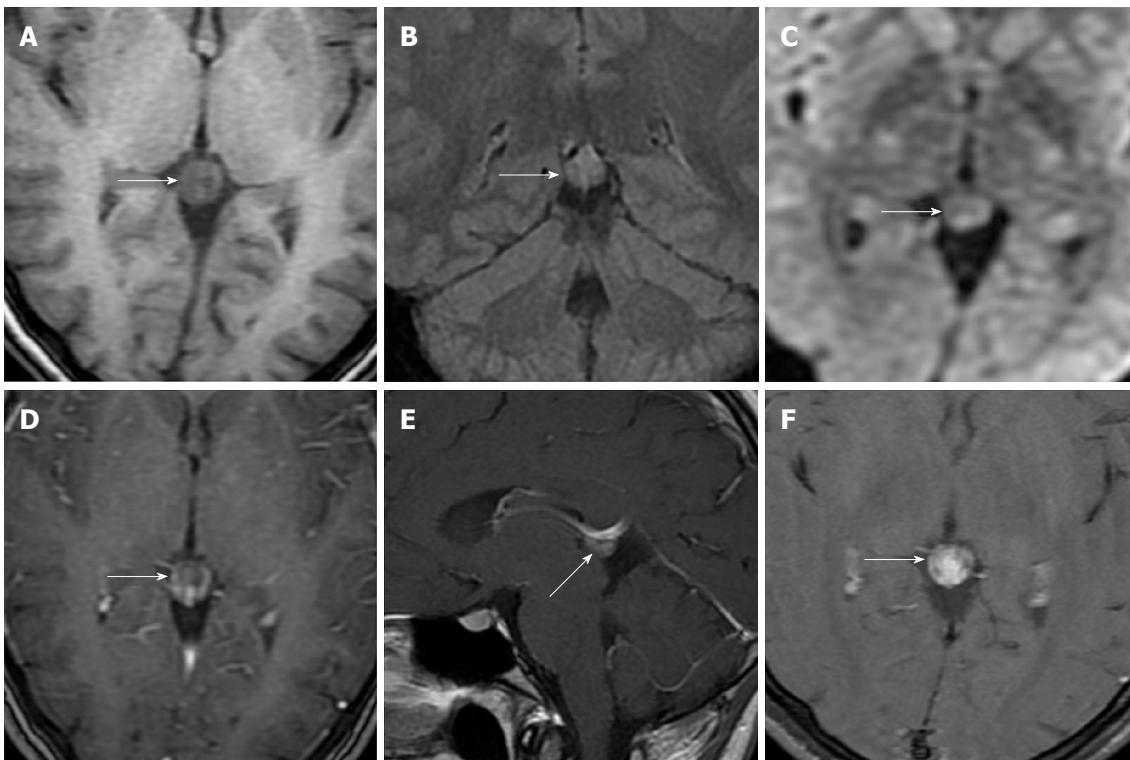| MRI features of pineal cysts	*n* (%)
Cyst type	
Typical	35 (62.50)
Atypical	21 (37.50)
Two or more septation-loculation	18 (32.14)
Contour lobularity	11 (19.64)
Cyst contrast-enhancement	21
Peripheral rim enhancement	15 (71.42)
Peripheral rim and septal enhancement	3 (14.28)
Partial rim enhancement	2 (9.52)
Dense heterogeneous enhancement	1 (4.76)
Cyst intensity relative to CSF on T2 weighted images	
Isointense	55 (98.21)
Hyperintense	1 (1.79)
Cyst intensity relative to CSF on T1 weighted images	
Isointense	53 (94.64)
Hyperintense	3 (5.36)
Cyst intensity relative to CSF on FLAIR images	
Isointense	6 (10.71)
Hyperintense	50 (89.29)
Diffusion restriction	0

MRI: Magnetic resonance imaging; CSF: Cerebrospinal fluid; FLAIR: Fluid-attenuated inversion recovery.

PCs which were monitored by follow-up examinations ($P > 0.05$). Initial dimensions and volumes of PCs and observed changes during the follow-up period are given in Table 5.

DISCUSSION

PC are observed in 0.6-10.8% of all random or consecutive brain MRI studies[5,11-14] and in 23% of healthy volunteers[15]. Al-Holou *et al*[16] found an incidence rate of 1.9% in an MRI study on a child population comprising 10821 children under 18 years of age. Lacroix-Boudhrioua *et al*[13] found a PC incidence rate of 11% in a high-resolution MRI study on a child patient group without a neurological indication. Considerable differences in reported PC incidence in MRI literature could be due to technical parameters or methodology (slice thickness, sequence type, strength of the magnetic field, size threshold of cysts included, *etc.*) as well as due to population differences (age, gender and race)[17]. In cadaver autopsies, pineal cyst incidence of up to 40% have been reported[5,18]. Higher incidence in autopsy series could be explained by the fact that small sized cysts of 2-5 mm can be detected only in cadaveric studies[13]. In the present study, only six of the 1327 patients (0.4%) who were 17 years of age and under were found to have PC. Frequency of PC in all ages combined was 0.58%, which was lower than the incidence rates reported in literature. Lower incidence rate in the present study could be due to population difference.

Al-Holou *et al*[12] found a prevalence of 2.0% in an adult population in the range of 19-30 years of age. Sawamura *et al*[19] reported a decrease in PC incidence after the age of 40. Al-Holou *et al*[12], on the other hand,

mentioned that PC prevalence peaked at late childhood period and then started to decrease in adult age range. Most studies in literature reported lower PC incidence rates in infants and in old ages (older adults)[4,6,12,16,20-22]. In the present study, no PC was observed in infantile period, and the incidence of PC tended to increase towards the end of the second decade and peaked at the fourth decade. A slight decrease in prevalence was observed at the fifth decade, but the decrease in older ages was more pronounced.

There are many studies in literature reporting higher incidence of PCs in women[12,14,16,19]. Studying a population of children and young adults, Al-Holou *et al*[16] mentioned PC frequency of 2.4% in women and 1.5% in men. In a retrospective study by Al-Holou *et al*[12] carried out on 48417 patients who had brain MRI, frequency of pineal cyst was reported to be 1.1% in women and 0.8% in men. Similarly, Sawamura *et al*[19] found PC incidence rates of 1.6% for women and 0.96% for men. In the present study, on the other hand, relatively lower incidence rates of PC were observed, women having higher incidence rates (0.8%) than men (0.3%) similar to literature.

Most PCs are small sized[1,2]. Barboriak *et al*[4] reported that average PC diameter was 11.2 mm and volume was 1.42 cm^3. They also reported that 47% of PCs had 10 mm or smaller maximum linear dimension. Nevins *et al*[14] evaluated 281 PC, and found that median size of PCs at diagnosis was 10 mm. Al-Holou *et al*[12] found that starting dimensions of PCs were 9.7 ± 3.8 mm in sagittal anteroposterior, 6.8 ± 2.9 mm in sagittal craniocaudal and 7.0 ± 2.8 mm in axial width dimensions, and that 50% of PCs had less than 10 mm of maximum size. The authors also mentioned that sizes of PC in women and men were not significantly different, and volume of PCs was not significantly associated with age. Average PC dimension in the present study was 10.07 ± 2.93 mm in all planes (AP, ML and CC dimensions). Maximum dimension was less than 10 mm in 37.5% of PCs ($n = 21$), which was somewhat lower than what was reported in literature. This may be due to different measurement techniques used to determine PC dimensions. PC volumes in the present study were not significantly associated with gender or age of the patients ($P = 0.74$ and $P = 0.81$, respectively).

PCs typically have a benign prognosis, but some studies reported rare size changes of PCs over time[4,12,23]. Tamaki *et al*[7] and Golzarian *et al*[6] reported that size of PCs did not change in follow-up examinations. Al-Holou *et al*[12] found that only 2.6% of PCs which were monitored for periods varying from 6 mo to 3 years had an average maximum diameter increase of 3.5 mm, while size decreased in 15% and remained stable in 82% of them. In 32 patients monitored for periods ranging from six months to nine years, Barboriak *et al*[4] observed that maximal size did not change in 75.0% of PCs, 2-4 mm size decreases were observed in 9.37%, and 2-3 mm size increases were observed in 6.25% of

Table 5 Iinitial dimensions and volumes and subsequent changes of pineal cysts

Pineal cyst dimensions and volume	Value (range)
Minimal-maximal linear dimension	5.0-19.70 mm
All plane mean dimension (AP, ML, CC)	10.07 ± 2.93 mm
Cyst volume (mean ± SD, range)	0.62 ± 0.54 (0.11-3.35) cm³
Cyst dimension (mean ± SD, range) (mm)	
Anteroposterior (AP)	11.18 ± 3.03 (6.50-19.00)
Mediolateral (ML)	10.41 ± 2.72 (5.80-19.70)
Craniocaudal (CC)	8.63 ± 2.47 (5.0-18.30)
Changes in dimensions during follow-up period (mean ± SD, range) (mm)	
Anteroposterior (AP)	-0.08 ± 0.53 (-1.60-0.7)
Mediolateral (ML)	-0.22 ± 0.87 (-3-0.8)
Craniocaudal (CC)	0.16 ± 0.56 (-0.70-1.40)

the PCs. On the other hand, they also found that two cysts resolved completely, and a new cyst developed and grew to 12 mm. Nevins *et al*[14] reported that only 11 of the 181 PC that they followed for periods varying from 1 to 68 mo had dimensional changes. Seven of them had a 2 mm median diameter increase and the other four had 2.5 mm median diameter decrease[14]. Of the 18 PCs which were monitored by follow-up examinations in the present study, three (16.66%) had no size change, while five (27.77%) had size increases in all dimensions, four (22.22%) had size decreases and six (33.33%) had both increase and decreases in at least one dimension. Average increase in maximum diameter was 0.64 ± 0.37 mm (range: 0.1-1.4 mm), and average decrease in maximum diameter was 0.62 ± 0.45 mm (range: 0.1-1.6 mm). Size changes in PCs were much lower than those in literature. Barboriak *et al*[4] reported that no significant difference was observed for average volumes and maximum linear dimensions of PCs in initial and final MRI screenings. In parallel with Barboriak *et al*[4], changes between initial and final sizes of PCs were not statistically significant in the present study ($P > 0.05$). Barboriak *et al*[4] mentioned that MRI monitoring of incidentally determined asymptomatic cysts are not practical and suggested that cysts with atypical imaging features should be monitored. Nevins *et al*[14] recommended a single follow-up MRI scan with gadolinium at 12 mo after diagnosis and discharge if the pineal cyst has not increased in size. It has been indicated that follow-up imaging and even tissue sampling could be necessary for a lesion which does not meet MRI criteria of a typical pineal cyst or which manifests itself with clinical symptoms[10]. Nevertheless, many benign PC were reported to have irregular nodular enhancement on MR images[9]. Fleege *et al*[9] reported that 14 of 19 pineal lesions confirmed through histological examinations had been preoperatively concluded to be pineal neoplasms. The authors noted that PC had the appearance of complex cysts and cysts with fluid levels, calcification, hemorrhage, and enhancement[9]. Similarly, Fain *et al*[24] found abnormal rim enhancement on intracranial imaging in 50% of benign cysts confirmed by histological examination. It has been proposed that this abnormal peripheral rim

enhancement could be associated with surrounding venous structures or displaced pineal gland[1,6,16]. Therefore, it was concluded that presence of a solid contrast-enhancement component in PC should be considered as a worrying appearance[5].

Radiological appearance of PCs changes by imaging modalities and parameters used. PCs are smooth-edged ovoid lesions which could generally be better visualized on sagittal plane in MRI. There are different reports in literature about signal properties of PCs obtained by different sequence parameters[6,19,21,25]. Osborn[26] indicated that almost all PCs appeared isointense or slightly intense with CSF on T2 weighted MR images, but on T1 weighted images, 50%-60% of them appeared slightly hyperintense compared to CSF, about 40% appeared isointense and 1%-2% with intracystic hemorrhage, on the other hand, appeared hyperintense. The author also reported that signal of most PCs was not completely suppressed on FLAIR images and appeared moderately hyperintense compared to brain parenchyma. Nevertheless, signal properties of PCs were found to vary depending upon its content, presence of hemorrhage and calcification[26]. More than 60%-90% of PCs were shown to have contrast-enhancement on contrast-enhanced series[1,2,26]. On diffusion MRI content of cyst typically does not have diffusion limitation[27]. Almost all PCs in the present study (98.21%) were isointense with CSF, and only one (1.79%) was slightly hyperintense on T2 weighted images. On T1 weighed series, 94.64% were isointense with CSF and only 5.36% was slightly hyperintense. On FLAIR series, 89.29% were hyperintense with CSF and 10.71% were isointense. Contrast-enhancement was observed in PCs of all patients who had contrast-enhanced examination. Barboriak *et al*[4] reported that only one cyst showed signal change on proton density weighted sequence during follow-up examinations. In the present study, no change was observed in MRI signal feature of any cyst in any sequence.

PCs were reported to have unilocular appearance in literature dealing with routine brain MRI studies[4,25]. Al-Holou *et al*[12], on the other hand, found that 11% of PCs had multicystic appearance or had atypical features due to abnormal contrasting. Jinkins *et al*[25]

mentioned that most PCs were unilocular but PCs in two patients had septation. Using FIESTA (fast imaging employing steady-state acquisition) sequence, Pastel *et al*[28] detected that six of the 10 PCs (60%) had internal septation or multiloculation. In their high-resolution MRI studies, Lacroix-Boudhrioua *et al*[13] found that 74% of PCs had septation. In addition, pathological studies reported multiple septations as common findings in PCs[12,18]. This fact means that majority of PC septations could not be detected in routine MRI series. In the present study, septation was observed in 18 PCs (32.14%). Three PCs which had been described as typical based on MRI exams before our MRI machine was upgraded (before 2017) were classified atypical in follow-up MRI exams carried out in 2017 and later due to observed internal septations. It was concluded that especially BRAVO sequence (high resolution three-dimensional T1-weighted gradient images) of isotropic 1 mm^3, both contrast-enhanced and without contrast-enhanced, improved the detection of internal septations. Studies in literature mentioned that growth and changing patterns of septated cysts are not significantly different from those of unilocular ones[5,12,28]. Similar to the studies in literature, no significant difference was observed between growth patterns of atypical and typical PCs ($P > 0.05$).

PCs are localized in pineal gland and may partly or completely occupy it. A typical pineal cyst shows a contrasting wall feature in a thin peripheral rim style of less than 2 millimeter[4]. Since there is no blood-brain barrier around pineal gland, contrast-enhancement is observed in cyst walls[11]. In the center of cyst, contrast-enhancement is not normally observed in images taken right after contrast matter administering. Nevertheless, in images taken 60-90 min later, cyst may have contrast-enhancement in a uniform and solid appearance[1]. In atypical PCs, findings such as internal septation or loculation, irregular nodular contrast-enhancement, edge lobulation and hemorrhage can be observed[1,4,11,16]. However, these atypical findings are not necessarily related to malignity or cyst enlargement[1]. In fact, high resolution MRI studies showed that internal septations and loculations can be detected in great majority of PCs[13,28]. Follow-up examinations in many studies, including the present one, showed that atypical PCs are not different from the typical ones in terms of size and natural change[4,12]. This finding suggests that internal septation-loculations or lobulations are in fact inherent in PCs and that typical-atypical classification based on these criteria should be reconsidered. Nevertheless, despite the advances in high resolution MRI, there are not definite radiological methods to distinguish benign PC from pineal region malignancies containing cystic components such as pineocytomas, pineoblastomas, germinomas or mature teratomas[29]. In addition, similar to pineal area tumors such as pineoblastomas, teratomas or pilocytic astrocytoma which look like large cysts, benign PCs which lead to intracystic hemorrhage and hydroc-

ephaly and have a complicated appearance may mimic malignant tumors[9,30]. Since malignancy possibility is higher in PCs which grow and have high contrast-enhancement and hemorrhage, more frequent follow-ups or neurosurgical intervention may be necessary with these PCs[29].

PC could enlarge in time due to both intracystic fluid increase and hemorrhage and become symptomatic. Because of their mass effect on midbrain next to them, PCs could lead to Parinaud syndrome (paralysis of upward gaze, retraction in eyelid and abnormal pupil reactions)[31,32]. Sudden death events have been reported because of intra-cystic hemorrhage, also called pineal apoplexy, and acute hydrocephaly[33,34]. PCs with diameters smaller than 10 mm typically do not exert compression on adjacent structures such as cerebral aqueduct, vein of Galen, and the quadrigeminal plate, and they are frequently asymptomatic[1,20]. However, PCs with diameters larger than 15 mm could make local mass effect on adjacent structures and lead to neurological symptoms as a result of hydrocephaly due to compression of cerebral aqueduct[1]. Although there were seven PCs with maximum diameter of more than 15 mm in the present study, gross local mass effect or cerebral aqueduct compression was not observed in any patient. Patients may have a large scale of symptoms due to PC, headache being the most common. Other frequently observed symptoms in PC patients are seizures, dizziness, blurred vision, hemiparesis and vomiting[29]. Previously, headache in these patients were thought to be due to increased intracranial pressure. However, recent studies indicated a hormonal imbalance indicating melatonin as culprit[29,35]. In addition, a recent study reported that MR biomarkers (tectum-splenium-cyst ratio and thalamic and periventricular edema) could be associated with central venous hypertension and severity of symptoms in non-hydrocephalic, symptomatic PC patients[36]. Although PCs did not lead to clear compression findings in the present study, the most common symptom experienced by the patients was headache (75%).

Asymptomatic cysts could be accompanied by tectal deformities of different intensities[4]. Although higher deformity levels are observed in larger cysts as expected, Barboriak *et al*[4] reported that they could not obtain any finding indicating that cysts with higher level of deformities could further enlarge in follow-up examinations. Some studies reported hydrocephaly in patients with PCs larger than 20 mm[37]. On the other hand, Barboriak *et al*[4] found that only a moderate enlargement in ventricle was observed in two patients with PCs of that size. No patients had cysts with maximum diameter of more than 20 mm diameter, and hydrocephaly due to the mass effect of PC was not observed in any patient in the present study.

Because of the uncertainties about the natural history of PC, especially about asymptomatic ones, there is no consensus in the literature about what is the most appropriate treatment approach for PC[29].

Management options for asymptomatic cysts vary from total ignoring even without any follow-ups to surgical intervention. Surgical intervention is commonly refrained in asymptomatic patients[29]. Some clinicians suggest yearly follow-ups using clinical examination and imaging, but others do not recommend routine imaging for known PC[12,29]. Similarly, while some studies highly recommended routine clinical examinations and imaging in children[16,23,29,31], others considered PCs as common incidental findings and suggested no follow-ups or contrast-enhanced examinations for children without any neurological indications[13]. In symptomatic patients, especially in ones with hydrocephaly, surgical interventions such as shunt placement, cyst excision, endoscopic or stereotactic aspiration, and endoscopic third ventriculostomy could be preferred[29,38]. In their review paper, Májovský *et al*[39] reported positive feedbacks for elimination of symptoms after PC surgery in most symptomatic patients and even in patients with non-specific symptoms. Although the authors considered microsurgical resection of PCs, using supracerebellar-infratentorial approach, as a viable option for symptomatic patients, they noted that this suggestion was based on limited number of reports[39].

The present study has some limitations. First, relatively fewer PC were evaluated retrospectively in the present study. Second, only 21 of the patients (37.5%) had contrast-enhanced examination. Third, the number of cases with follow-ups was few and follow-up periods were not standard for patients who had them. Fourth, none of the patients had histopathological examinations. Finally, quite small size increase or decrease was observed in a small number of PC. Although we are confident that the change in size is accurate, there is a slight possibility that some of the changes may reflect measurement error.

In conclusion, PCs are cysts which do not have marked dimensional and natural changes. Their frequency is higher in women and adults, and their sizes are not associated with gender or age. Great majority of them are isointense with CSF on T1 and T2A series. On FLAIR sequence, they are hyperintense compared to CSF, and they may be smoothly contoured, unilocular or multilocular. Typical ones may have contrast-enhancement in peripheral rim style, while multilocular ones may have septal contrast-enhancement.

ARTICLE HIGHLIGHTS

Research background
Pineal cysts (PC) are cysts which are frequently detected incidentally in brain magnetic resonance imaging (MRI). No clear consensus has been reached yet over the classification and follow-up procedures in routine clinical practice. PCs were classified based on MRI findings in the present study. Unilocular, smooth edged, ovoid PCs with homogenous interior structure and less than 2 mm wall thickness were considered typical PC, while multilocular PCs with walls thicker than 2 mm, septation or contour lobulation were considered atypical. In addition, size and natural changes in follow-up examinations were also investigated.

Research motivation
Lack of a consensus over radiological classification and follow-up of PC, and

their radiological findings that resemble other lesions of pineal area create difficulties. Presentation of radiological studies dealing with PCs in different population including follow-up images taken at different series could help to resolve this uncertainty.

Research objectives
In the present study, PCs detected using brain MRI examinations in our population were classified based on radiological imaging features. In addition, whether PCs had significant size or nature changes were also evaluated.

Research methods
A total of 9546 patients who had brain MRI examination in March 2010-January 2018 period were studied retrospectively for the presence of PCs. Sizes in three dimensions, volumes, contours, signal intensities, internal septation or loculation features and contrasting patterns of PCs were evaluated. Size and natural changes of PCs were investigated in patients during follow-up examinations with durations varying from 2 to 96 mo. Associations between PC frequency and gender, between PC volumes and gender and age, and amount of changes between initial and final sizes of PCs were statistically analyzed.

Research results
Fifty-six patients (44 female and 12 male) were found to have had PC. Age range of patients with PC was 5-61 (mean: 31.26 ± 12.73). Frequency of PC was 0.58%. PC incidence rates were significantly different in men and women. In terms of classification, 62.50% of the PCs were typical and 37.50% were atypical. Average PC sizes were 11.18 ± 3.03 mm in AP, 10.41 ± 2.72 mm in ML and 8.63 ± 2.47 mm in CC directions. Natural change was not observed in any PC with follow-ups. Average dimension changes in PCs with follow-ups were (-0.08 ± 0.53) mm, (-0.22 ± 0.87) mm, and (0.16 ± 0.56) mm in AP, ML and CC dimension, respectively. No significant difference was found between initial and final sizes of PCs which were monitored by follow-up examinations.

Research conclusions
It was revealed in the present study that classification of PCs concluded to be unilocular (*i.e.*, typical) based on routine MRI sequences could change to atypical when high resolution sequences indicated internal septations. No significant size or natural change was observed in follow-up examinations of PCs. Therefore, it could be suggested that asymptomatic PCs which do not show any size or natural changes during one- or two-year follow-ups should be removed from routine follow-up.

Research perspectives
The present study showed that PCs are cysts frequently observed as incidental lesions in brain MRI series, that they have an average diameter of 10 mm and that they have signal features similar to CSF in T1 and T2 weighed series while giving higher signal intensities than CSF in FLAIR sequence. In addition, it was revealed that typical or atypical classification of PCs could change based on resolution of sequence used in identification of PCs. Elimination of frequent follow-ups of asymptomatic PCs could lower cost and labor burden on health care system.

REFERENCES

1 **Choy W**, Kim W, Spasic M, Voth B, Yew A, Yang I. Pineal cyst: a review of clinical and radiological features. *Neurosurg Clin N Am* 2011; **22**: 341-351, vii [PMID: 21801982 DOI: 10.1016/j.nec.2011.06.001]

2 **Osborn AG**, Preece MT. Intracranial cysts: radiologic-pathologic correlation and imaging approach. *Radiology* 2006; **239**: 650-664 [PMID: 16714456 DOI: 10.1148/radiol.2393050823]

3 **Kahilogullari G**, Massimi L, Di Rocco C. Pineal cysts in children: case-based update. *Childs Nerv Syst* 2013; **29**: 753-760 [PMID: 23283557 DOI: 10.1007/s00381-012-2011-6]

4 **Barboriak DP**, Lee L, Provenzale JM. Serial MR imaging of pineal cysts: implications for natural history and follow-up. *AJR Am J Roentgenol* 2001; **176**: 737-743 [PMID: 11222216 DOI: 10.2214/ajr.176.3.1760737]

5 **Cauley KA**, Linnell GJ, Braff SP, Filippi CG. Serial follow-up MRI of indeterminate cystic lesions of the pineal region: experience at a

rural tertiary care referral center. *AJR Am J Roentgenol* 2009; **193**: 533-537 [PMID: 19620453 DOI: 10.2214/AJR.08.1906]

6   **Golzarian J**, Balériaux D, Bank WO, Matos C, Flament-Durand J. Pineal cyst: normal or pathological? *Neuroradiology* 1993; **35**: 251-253 [PMID: 8492885 DOI: 10.1007/BF00602604]

7   **Tamaki N**, Shirataki K, Lin TK, Masumura M, Katayama S, Matsumoto S. Cysts of the pineal gland. A new clinical entity to be distinguished from tumors of the pineal region. *Childs Nerv Syst* 1989; **5**: 172-176 [PMID: 2758432 DOI: 10.1007/BF00272122]

8   **Hayashida Y**, Hirai T, Korogi Y, Kochi M, Maruyama N, Yamura M, Yamashita Y. Pineal cystic germinoma with syncytiotrophoblastic giant cells mimicking MR imaging findings of a pineal cyst. *AJNR Am J Neuroradiol* 2004; **25**: 1538-1540 [PMID: 15502133]

9   **Fleege MA**, Miller GM, Fletcher GP, Fain JS, Scheithauer BW. Benign glial cysts of the pineal gland: unusual imaging characteristics with histologic correlation. *AJNR Am J Neuroradiol* 1994; **15**: 161-166 [PMID: 8141049]

10   **Fakhran S**, Escott EJ. Pineocytoma mimicking a pineal cyst on imaging: true diagnostic dilemma or a case of incomplete imaging? *AJNR Am J Neuroradiol* 2008; **29**: 159-163 [PMID: 17925371 DOI: 10.3174/ajnr.A0750]

11   **Mamourian AC**, Towfighi J. Pineal cysts: MR imaging. *AJNR Am J Neuroradiol* 1986; **7**: 1081-1086 [PMID: 3098073]

12   **Al-Holou WN**, Terman SW, Kilburg C, Garton HJ, Muraszko KM, Chandler WF, Ibrahim M, Maher CO. Prevalence and natural history of pineal cysts in adults. *J Neurosurg* 2011; **115**: 1106-1114 [PMID: 21780858 DOI: 10.3171/2011.6.JNS11506]

13   **Lacroix-Boudhrioua V**, Linglart A, Ancel PY, Falip C, Bougnères PF, Adamsbaum C. Pineal cysts in children. *Insights Imaging* 2011; **2**: 671-678 [PMID: 22347985 DOI: 10.1007/s13244-011-0117-0]

14   **Nevins EJ**, Das K, Bhojak M, Pinto RS, Hoque MN, Jenkinson MD, Chavredakis E. Incidental Pineal Cysts: Is Surveillance Necessary? *World Neurosurg* 2016; **90**: 96-102 [PMID: 26944882 DOI: 10.1016/j.wneu.2016.02.092]

15   **Pu Y**, Mahankali S, Hou J, Li J, Lancaster JL, Gao JH, Appelbaum DE, Fox PT. High prevalence of pineal cysts in healthy adults demonstrated by high-resolution, noncontrast brain MR imaging. *AJNR Am J Neuroradiol* 2007; **28**: 1706-1709 [PMID: 17885233 DOI: 10.3174/ajnr.A0656]

16   **Al-Holou WN**, Garton HJ, Muraszko KM, Ibrahim M, Maher CO. Prevalence of pineal cysts in children and young adults. Clinical article. *J Neurosurg Pediatr* 2009; **4**: 230-236 [PMID: 19772406 DOI: 10.3171/2009.4.PEDS0951]

17   **Jussila MP**, Olsén P, Salokorpi N, Suo-Palosaari M. Follow-up of pineal cysts in children: is it necessary? *Neuroradiology* 2017; **59**: 1265-1273 [PMID: 28942520 DOI: 10.1007/s00234-017-1926-8]

18   **Hasegawa A**, Ohtsubo K, Mori W. Pineal gland in old age; quantitative and qualitative morphological study of 168 human autopsy cases. *Brain Res* 1987; **409**: 343-349 [PMID: 3580881 DOI: 10.1016/0006-8993(87)90720-7]

19   **Sawamura Y**, Ikeda J, Ozawa M, Minoshima Y, Saito H, Abe H. Magnetic resonance images reveal a high incidence of asymptomatic pineal cysts in young women. *Neurosurgery* 1995; **37**: 11-15; discussion 15-16 [PMID: 8587669 DOI: 10.1227/00006123-199507000-00002]

20   **Sener RN**. The pineal gland: a comparative MR imaging study in children and adults with respect to normal anatomical variations and pineal cysts. *Pediatr Radiol* 1995; **25**: 245-248 [PMID: 7567225 DOI: 10.1007/BF02011087]

21   **Lee DH**, Norman D, Newton TH. MR imaging of pineal cysts. *J Comput Assist Tomogr* 1987; **11**: 586-590 [PMID: 3597879 DOI: 10.1097/00004728-198707000-00005]

22   **Lum GB**, Williams JP, Machen BC, Akkaraju V. Benign cystic pineal lesions by magnetic resonance imaging. *J Comput Tomogr* 1987; **11**: 228-235 [PMID: 3608546 DOI: 10.1016/0149-936X(87)90087-7]

23   **Mandera M**, Marcol W, Bierzyńska-Macyszyn G, Kluczewska E. Pineal cysts in childhood. *Childs Nerv Syst* 2003; **19**: 750-755 [PMID: 12920545 DOI: 10.1007/s00381-003-0813-2]

24   **Fain JS**, Tomlinson FH, Scheithauer BW, Parisi JE, Fletcher GP, Kelly PJ, Miller GM. Symptomatic glial cysts of the pineal gland. *J Neurosurg* 1994; **80**: 454-460 [PMID: 8113858 DOI: 10.3171/jns.1994.80.3.0454]

25   **Jinkins JR**, Xiong L, Reiter RJ. The midline pineal "eye": MR and CT characteristics of the pineal gland with and without benign cyst formation. *J Pineal Res* 1995; **19**: 64-71 [PMID: 8609598 DOI: 10.1111/j.1600-079X.1995.tb00172.x]

26   **Osborn AG**. Osborn's Brain: Imaging, Pathology, and Anatomy. 1st ed. Canada: Amirsys, 2013: 788-791

27   **Fang AS**, Meyers SP. Magnetic resonance imaging of pineal region tumours. *Insights Imaging* 2013; **4**: 369-382 [PMID: 23640020 DOI: 10.1007/s13244-013-0248-6]

28   **Pastel DA**, Mamourian AC, Duhaime AC. Internal structure in pineal cysts on high-resolution magnetic resonance imaging: not a sign of malignancy. *J Neurosurg Pediatr* 2009; **4**: 81-84 [PMID: 19569915 DOI: 10.3171/2008.5.17681]

29   **Starke RM**, Cappuzzo JM, Erickson NJ, Sherman JH. Pineal cysts and other pineal region malignancies: determining factors predictive of hydrocephalus and malignancy. *J Neurosurg* 2017; **127**: 249-254 [PMID: 27767399 DOI: 10.3171/2016.8.JNS16220]

30   **Sarikaya-Seiwert S**, Turowski B, Hänggi D, Janssen G, Steiger HJ, Stummer W. Symptomatic intracystic hemorrhage in pineal cysts. Report of 3 cases. *J Neurosurg Pediatr* 2009; **4**: 130-136 [PMID: 19645546 DOI: 10.3171/2009.4.PEDS08309]

31   **Wisoff JH**, Epstein F. Surgical management of symptomatic pineal cysts. *J Neurosurg* 1992; **77**: 896-900 [PMID: 1432132 DOI: 10.3171/jns.1992.77.6.0896]

32   **Ramji S**, Touska P, Rich P, MacKinnon AD. Normal neuroanatomical variants that may be misinterpreted as disease entities. *Clin Radiol* 2017; **72**: 810-825 [PMID: 28747250 DOI: 10.1016/j.crad.2017.06.118]

33   **Milroy CM**, Smith CL. Sudden death due to a glial cyst of the pineal gland. *J Clin Pathol* 1996; **49**: 267-269 [PMID: 8675746 DOI: 10.1136/jcp.49.3.267]

34   **Richardson JK**, Hirsch CS. Sudden, unexpected death due to "pineal apoplexy". *Am J Forensic Med Pathol* 1986; **7**: 64-68 [PMID: 3728423 DOI: 10.1097/00000433-198603000-00014]

35   **Peres MF**. Melatonin, the pineal gland and their implications for headache disorders. *Cephalalgia* 2005; **25**: 403-411 [PMID: 15910564 DOI: 10.1111/j.1468-2982.2005.00889.x]

36   **Eide PK**, Pripp AH, Ringstad GA. Magnetic resonance imaging biomarkers indicate a central venous hypertension syndrome in patients with symptomatic pineal cysts. *J Neurol Sci* 2016; **363**: 207-216 [PMID: 27000252 DOI: 10.1016/j.jns.2016.02.038]

37   **Fetell MR**, Bruce JN, Burke AM, Cross DT, Torres RA, Powers JM, Stein BM. Non-neoplastic pineal cysts. *Neurology* 1991; **41**: 1034-1040 [PMID: 2067630 DOI: 10.1212/WNL.41.7.1034]

38   **Berhouma M**, Ni H, Delabar V, Tahhan N, Memou Salem S, Mottolese C, Vallee B. Update on the management of pineal cysts: Case series and a review of the literature. *Neurochirurgie* 2015; **61**: 201-207 [PMID: 24907165 DOI: 10.1016/j.neuchi.2013.08.010]

39   **Májovský M**, Netuka D, Beneš V. Is surgery for pineal cysts safe and effective? Short review. *Neurosurg Rev* 2018; **41**: 119-124 [PMID: 28702847 DOI: 10.1007/s10143-017-0876-2]

Obesity and pericallosal lipoma in X-linked emery-dreifuss muscular dystrophy: A case report - Does Emerin play a role in adipocyte differentiation?

Fabio Spanu, Luca Saba

Fabio Spanu, Luca Saba, Department of Radiology, Azienda Ospedaliero Universitaria, Cagliari 09045, Italy

ORCID number: Fabio Spanu (0000-0003-3765-3905); Luca Saba (0000-0003-2870-3771).

Correspondence to: Fabio Spanu, MD, Surgeon, Department of Radiology, Azienda Ospedaliero Universitaria, Polo di Monserrato s.s. 554 Monserrato, Cagliari 09045, Italy. docfabio.spanu@gmail.com
Telephone: +39-705-1096242
Fax: +39-705-6092299

Abstract

Emery dreifuss muscular dystrophy (EDMD) is a rare genetic syndrome consisting of tendon retractions, progressive muscle atrophy and cardiac involvement. We report a case of an obese patient affected by the familial X-linked form in which a pericallosal lipoma was found during investigation for a suspected acute vasculopathy. To date, EDMD has never been associated with cerebral lipomas and the X-linked form was never considered to be involved in lipodystrophic syndromes or non-muscular conditions. Our case confirms the variable expressivity of the disease and suggests a possible role of Emerin in the intranuclear regulation of signals for adipocyte cell differentiation.

Key words: Familiar emery dreifuss muscular dystrophy; Emerin; Adipocyte differentiation; Pericallosal lipoma; Emery-dreifuss-distrophy

Core tip: To date, emery dreifuss muscular dystrophy has never been associated with cerebral lipomas, and the X-linked form was never considered to be involved in extra-muscular syndromes. We presented a case of a patient affected by the X-linked form with a particular adipose tissue distribution and a cerebral and spinal lipoma, thus suggesting a possible role of Emerin in the intranuclear regulation of signals for cell differentiation, or in lipidic intracellular dysmetabolism when absent.

Spanu F, Saba L. Obesity and pericallosal lipoma in X-linked emery-dreifuss muscular dystrophy: A case report - Does Emerin play a role in adipocyte differentiation? *World J Radiol* 2018; 10(7): 78-82 Available from: URL: http://www.wjgnet.com/1949-8470/full/v10/i7/78.htm DOI: http://dx.doi.org/10.4329/wjr.v10.i7.78

INTRODUCTION

Emery dreifuss muscular dystrophy (EDMD) is a rare genetic syndrome described for the first time in 1966 after studying families with slowly progressive muscular dystrophy compared to the Duchenne-type[1]. It belongs to the group of nuclear envelopathies, defects in proteins that make up the nuclear envelope. However, even when included among the subgroup of laminopathies, not all the pathogenic variants in EDMD show defects in lamins. Specifically, in the X-linked EDMD variant, the protein Emerin, normally ubiquitously expressed on the nuclear membrane, is absent in 95% of individuals[2]. This form has a similar clinical picture compared to the autosomal dominant variant (involving Lamin A/C)[3], although not exactly the same, and is characterized by joint contractures (usually the first sign), slow and progressive muscle weakness (appearing first in AD variants), and cardiac involvement with arrhythmias and dilated cardiomyopathies[4]. Most of emerinopathies are null variants, but the phenotype may show intra-familial variability. Nevertheless, in contrast to mutations in the *Lamin A/C* gene, XL-EDMDs are not associated with Dunnigan-type familial partial lipodystrophy nor with cerebral involvement, including the occurrence of intracranial lipomas[5].

CASE REPORT

A 27-year-old man with Emery-Dreifuss muscular dystrophy presented at E.D. three hours after the onset of objective vertigo, followed by painful left arm weakness. He was from a family with four brothers affected by the X-linked form of the disease, due to the 130 C > T (Q44X) non-sense mutation in the exon 2 of the *EMD* gene. He was obese, with a particular accumulation of facial and neck adipose tissue. He was pharmacologically treated with ramipril, bisoprolol and apixaban for cardiac rhythm disorders, monitored with a loop recorder reveal. His medical history revealed several episodes of aberrant intraventricular conduction followed by SVPT, with isolated episodes of bradycardia and atrial ectopic beats. Echocardiograms had shown bi-atrial and LV enlargement. Muscular involvement was moderate, with deterioration of medial head of gastrocnemius, semimembranosus and, although mildly, lateral head of gastrocnemius, vasti, adductor magnus and long head of biceps femoris. No clear deformities or contractures were evident, in contrast to the patient's two affected younger brothers and an affected first-grade cousin.

The clinical exam at the E.D. showed a left arm downward drift associated with local joint pain. The patient was alert, oriented and cooperative, and the thoracic and abdominal clinical evaluation showed normal findings. Suspecting an acute vasculopathy, he underwent an urgent head NCCT that revealed the presence of a left-sided hypodense peri-callosal curvilinear lesion (Figure 1). No clear cerebral ischemic signs were observed. Further CT Angiography showed the perilesional course of pericallosal arteries below the rostrum and the genu of the corpus callosum, where both were pushed to the right side of the lesion and upward, resulting (above the lesion) in a correspondence between the body and splenium of the corpus callosum (Figure 2). The left artery narrowed progressively when compared to the contralateral. Furthermore, the exam ruled out vascular obstructions. The scan at thoracic level revealed a lesion with similar density and characteristics at the T1-T2 level, posterior to the cord and occupying the extradural space (Figure 3) with apparent dural impression. Then, the patient was admitted at the ward and was subjected to an MRI the next day, which did not show diffusivity alterations, thus definitely excluding areas of ischemia. Along the pericallosal region from rostrum to splenium, the lesion described in the CT appeared hyperintense at T1-W and long TR sequences, and hypointense at fat suppression sequences, without contrast enhancement and with clearly defined limits (Figure 4). These findings confirmed the initial hypothesis of a complete, left-sided, curvilinear pericallosal lipoma. Callosal aplasia was not observed. The day after, the patient's pain was subsiding with painkillers, while his weakened arm had completely recovered, allowing him to be discharged to his home.

DISCUSSION

EDMD is a rare genetic disease with an estimated prevalence of 0.13:100000-0.2:100000 overall[6], and of 1:100000 inhabitants for the XL-EDMD variant[7]. We reported a case of XL-EDMD in a family of five members affected, and a sister carrier of the same mutation c.130 C < T (pQ44X), in exon 2 of the *EMD* or *STA* genes. This mutation inserts a stop at codon 44, causing early translation termination of Emerin, resulting in C-terminal truncation and *in vivo* destabilization with complete loss[8].

Emerin is a type 2 integral membrane protein of 29-kDa, a resident of the inner nuclear membrane (INM) that is closely linked to lamin proteins, components of the nuclear lamina. It has been observed that in cells lacking a functional A-type lamin gene, as is observed in AD-EDMD, Emerin is largely mislocalized to the peripheral endoplasmic reticulum (ER). It has been postulated that the nuclear lamina plays a crucial role in limiting the segregation of INM proteins to the outer nuclear membrane and peripheral ER[9]. The tissue-specificity associated with laminopathies may be explained by a dysfunction in specific processes which take place in the ER, like cholesterol and fatty acid synthesis, due to the accumulation of proteins that are no longer contained within the nuclear envelope. This would result in aberrant adipocyte development and lipodystrophic diseases, as can be observed in Dunnigan-type familial partial lipodystrophy associated with mutations in the lamin *A/C* gene, characterized by selective loss of subcutaneous fat from the limbs and trunk, and its accumulation in

Figure 1 Paramedian left non-contrast computer tomography scan. This scan shows a curvilinear fat density lesion above the corpus callosum.
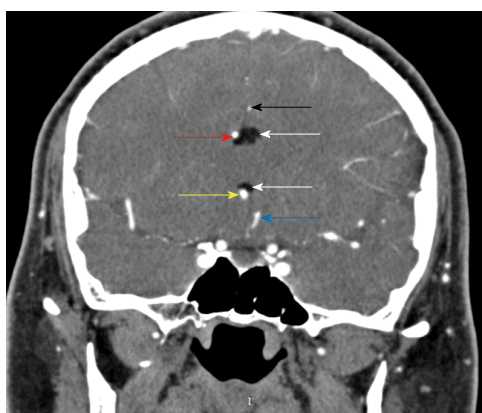

Figure 2 Coronal DSA. Shows the lipoma (white arrows), the right rostral A2 (yellow arrow), the right pericallosal artery (red arrow), the left rostral A2 (blue arrow), and the left pericallosal artery (black arrow).

Figure 3 Sagittal CT angiography. Shows two hypodense images compatible with lipomas within the extradural compartment, dorsal to the cord at the T1-T2 level.

Figure 4 T1-W 3D TFE + MDC magnetic resonance imaging. A: Showing the relationships between vasculature, corpus callosum, lipoma and adjacent brain tissues; B: Showing the pericallosal lesion, compatible with a complete curvilinear lipoma without callosal aplasia.

the face and neck[10]. Similarly, muscles and myocardium may suffer from an impaired Ca^{2+} release in the sarcoplasmic reticulum during contraction.

An alternative hypothesis suggests that the accumulation of nuclear envelope proteins in the ER could promote alterations in intracellular signaling pathways with effects on gene expression and cell survival[11]. Diff-
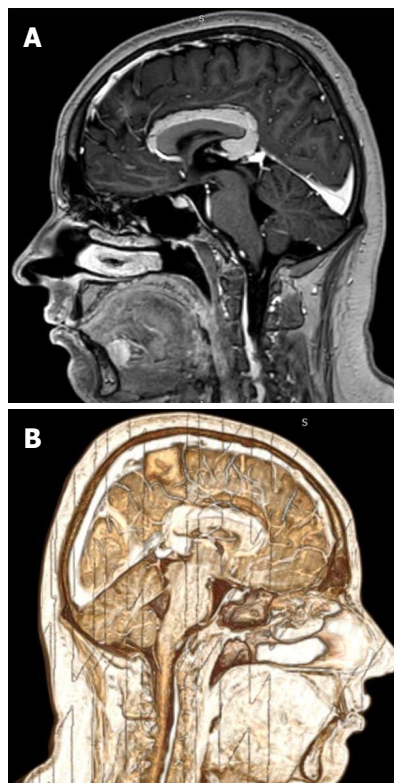
erent from laminopathies, Emerin in XL-EDMD is truncated at the C-terminus and is not detectable in the nuclear membrane. Thus, even if it is supposed to result in a more soluble form *in vitro*[12], the pathogenetic theory of accumulation seems less consistent.

Our patient showed a particular obese habitus, with accumulation of adipose tissue in the neck and facial districts with disproportionally leaner limbs. Evaluating the clinical course and the exams performed, the pericallosal and the spinal lipoma may be considered incidental findings, whereas the patient's symptoms could be related to an initial painful contracture that subsided after painkillers. Pericallosal are rare, fat-containing lesions, generally asymptomatic and accounting approximately for 0.1%-0.5% of all intracranial lesions[13]. Curvilinear and tubulonodular types have been described. Tubulonodular lipomas are considered more frequently associated with corpus callosum malformations[14], even if the series of Yilmaz *et al*[15] showed a stronger association with curvilinear lipomas. Our case is aligned with the classical association, which does not show clear morphological alterations in the corpus callosum. This may be important, since lipomas are considered as congenital malformations, and more often occur with cortical and callosal dysplasias and vascular malformations[16]. Nevertheless, Zettner and Netsky[17] pointed out that callosal dysgenesis are not the cause of lipomas, believing rather that the two conditions derive from two

distinct pathological processes, namely a meningeal mal-differentiation for lipomas and dysraphism for callosal abnormalities[17,18].

Finally, it is now clear that LEM domain proteins (such as LAP2B and Emerin) can interact with transcriptional regulators, playing a non-structural role in gene regulation. *In vitro* models speculate that Emerin binds A and B-type lamins as well as retinoblastoma (RB) proteins, which regulates the entry into S-phase and terminal differentiation, and at least four transcription factors, including germ-cell-less (GCL), BCL2-associated transcription factor (BTF) and barrier-to-autointegration factor (BAF)[19]. After binding Emerin, GCL acts on DP3-E2F by repressing its dependent gene expression, while BTF acts as a cell-death-promoting transcription repressor after binding a DNA-specific partner. BAF can bind directly to both Lamin A and Emerin, blocking GCL binding to Emerin, or can directly repress CRX-dependent genes *in vivo* after binding to double-stranded DNA. In muscle cells, Emerin binds several actin-binding proteins, including a nuclear isoform of Spectrin. This reinforces the lamina network by providing a further link between actin and protein 4.1, which is implicated in nuclei reconstruction after mitosis[19].

To date, EDMD has never been associated with cerebral lipomas, and the X-linked form was never considered to be involved in lipodystrophic syndromes or non-muscular conditions. Our case confirms the variable expressivity of the disease, and adds the suggestion of a possible role of Emerin in the intranuclear regulation of signals for adipocyte cell differentiation or lipidic intracellular metabolism in particular cell groups that are subject to specific and variable stimuli throughout a lifetime.

ARTICLE HIGHLIGHTS

Case characteristics
Spontaneous left arm weakness, objective vertigo, obesity.

Clinical diagnosis
Left arm downward drift associated with local joint pain.

Differential diagnosis
Acute vasculopathy; neuropathies; joint affections.

Laboratory diagnosis
Unremarkable laboratory examination.

Imaging diagnosis
A head NCCT revealed the presence of a left-sided hypodense peri-callosal curvilinear lesion; a CT Angiography ruled out vascular obstructions, while the thoracic scan showed two posterior extradural hypodense lesions at T1-T2. The MRI did not show diffusivity alterations: the curvilinear peri-callosal lesion appeared hyperintense in T1-W and hypointense at fat suppression sequences, without contrast enhancement, thus confirming the lipoma.

Treatment
Rest and painkillers.

Term explanation
Envelopathies: defects of proteins making up the nuclear envelope.

Experiences and lessons
A particular obesity pattern associated with cerebral-spinal lipomas may be related to the same gene defect in patients affected by the Emery-Dreifuss muscular dystrophy X-linked variant. In our case, lipomas may be considered incidental findings, whereas the patient's symptoms could be related to an initial painful contracture, which is a typical hallmark of the disease.

REFERENCES

1   **Emery AE**, Dreifuss FE. Unusual type of benign x-linked muscular dystrophy. *J Neurol Neurosurg Psychiatry* 1966; **29**: 338-342 [PMID: 5969090 DOI: 10.1136/jnnp.29.4.338]

2   **Yates JR**, Wehnert M. The Emery-Dreifuss Muscular Dystrophy Mutation Database. *Neuromuscul Disord* 1999; **9**: 199 [PMID: 10382916]

3   **Vytopil M**, Benedetti S, Ricci E, Galluzzi G, Dello Russo A, Merlini L, Boriani G, Gallina M, Morandi L, Politano L, Moggio M, Chiveri L, Hausmanova-Petrusewicz I, Ricotti R, Vohanka S, Toman J, Toniolo D. Mutation analysis of the lamin A/C gene (LMNA) among patients with different cardiomuscular phenotypes. *J Med Genet* 2003; **40**: e132 [PMID: 14684700 DOI: 10.1136/jmg.40.12.e132]

4   **Pasotti M**, Klersy C, Pilotto A, Marziliano N, Rapezzi C, Serio A, Mannarino S, Gambarin F, Favalli V, Grasso M, Agozzino M, Campana C, Gavazzi A, Febo O, Marini M, Landolina M, Mortara A, Piccolo G, Viganò M, Tavazzi L, Arbustini E. Long-term outcome and risk stratification in dilated cardiolaminopathies. *J Am Coll Cardiol* 2008; **52**: 1250-1260 [PMID: 18926329 DOI: 10.1016/j.jacc.2008.06.044]

5   **Shackleton S**, Lloyd DJ, Jackson SN, Evans R, Niermeijer MF, Singh BM, Schmidt H, Brabant G, Kumar S, Durrington PN, Gregory S, O'Rahilly S, Trembath RC. LMNA, encoding lamin A/C, is mutated in partial lipodystrophy. *Nat Genet* 2000; **24**: 153-156 [PMID: 10655060 DOI: 10.1038/72807]

6   **Norwood FL**, Harling C, Chinnery PF, Eagle M, Bushby K, Straub V. Prevalence of genetic muscle disease in Northern England: in-depth analysis of a muscle clinic population. *Brain* 2009; **132**: 3175-3186 [PMID: 19767415 DOI: 10.1093/brain/awp236]

7   **Bonne G**, Leturcq F, Ben Yaou R. Emery-Dreifuss Muscular Dystrophy. In: Adam MP, Ardinger HH, Pagon RA, Wallace SE, Bean LJH, Stephens K, Amemiya A, editors. SourceGeneReviews® [Internet]. Seattle (WA): University of Washington, Seattle; 1993-2018. 2004 Sep 29 [updated 2015 Nov 25]. [PMID: 20301609]

8   **Sullivan T**, Escalante-Alcalde D, Bhatt H, Anver M, Bhat N, Nagashima K, Stewart CL, Burke B. Loss of A-type lamin expression compromises nuclear envelope integrity leading to muscular dystrophy. *J Cell Biol* 1999; **147**: 913-920 [PMID: 10579712 DOI: 10.1083/jcb.147.5.913]

9   **Burke B**, Mounkes LC, Stewart CL. The nuclear envelope in muscular dystrophy and cardiovascular diseases. *Traffic* 2001; **2**: 675-683 [PMID: 11576443 DOI: 10.1034/j.1600-0854.2001.21001.x]

10 **Garg A**, Peshock RM, Fleckenstein JL. Adipose tissue distribution pattern in patients with familial partial lipodystrophy (Dunnigan variety). *J Clin Endocrinol Metab* 1999; **84**: 170-174 [PMID: 9920078 DOI: 10.1210/jcem.84.1.5383]

11 **Manilal S**, Recan D, Sewry CA, Hoeltzenbein M, Llense S, Leturcq F, Deburgrave N, Barbot J, Man N, Muntoni F, Wehnert M, Kaplan J, Morris GE. Mutations in Emery-Dreifuss muscular dystrophy and their effects on emerin protein expression. *Hum Mol Genet* 1998; **7**: 855-864 [PMID: 9536090 DOI: 10.1093/hmg/7.5.855]

12 **Pahl HL**, Baeuerle PA. The ER-overload response: activation of NF-kappa B. *Trends Biochem Sci* 1997; **22**: 63-67 [PMID: 9048485 DOI: 10.1016/S0968-0004(96)10073-6]

13 **Seidl Z**, Vaneckova M, Vitak T. Intracranial lipomas: a retros-

pective study. *Neuroradiol J* 2007; **20**: 30-36 [PMID: 24299585 DOI: 10.1177/197140090702000104]

14   **Yildiz H**, Hakyemez B, Koroglu M, Yesildag A, Baykal B. Intracranial lipomas: importance of localization. *Neuroradiology* 2006; **48**: 1-7 [PMID: 16237548 DOI: 10.1007/s00234-005-0001-z]

15   **Yilmaz MB**, Genc A, Egemen E, Yilmaz S, Tekiner A. Pericallosal Lipomas: A Series of 10 Cases with Clinical and Radiological Features. *Turk Neurosurg* 2016; **26**: 364-368 [PMID: 27161462 DOI: 10.5137/1019-5149.JTN.13008-14.0]

16   **Jiménez Caballero PE**. Interhemispheric lipoma associated with agenesis of the corpus callosum. *Neurologia* 2012; **27**: 515-517

[PMID: 21890243 DOI: 10.1016/j.nrl.2011.07.008]

17   **Zettner A**, Netsky MG. Lipoma of the corpus callosum. *J Neuropathol Exp Neurol* 1960; **19**: 305-319 [PMID: 13847327 DOI: 10.1097/00005072-196004000-00010]

18   **Wallace D**. Lipoma of the corpus callosum. *J Neurol Neurosurg Psychiatry* 1976; **39**: 1179-1185 [PMID: 1011028 DOI: 10.1136/jnnp.39.12.1179]

19   **Cohen M**, Lee KK, Wilson KL, Gruenbaum Y. Transcriptional repression, apoptosis, human disease and the functional evolution of the nuclear lamina. *Trends Biochem Sci* 2001; **26**: 41-47 [PMID: 11165516 DOI: 10.1016/S0968-0004(00)01727-8]